

## Dissociative ionization of benzene in intense laser fields of picosecond duration

V. R. Bhardwaj, K. Vijayalakshmi, and D. Mathur

*Tata Institute of Fundamental Research, Homi Bhabha Road, Mumbai 400 005, India*

(Received 19 August 1998)

Mass spectrometry experiments have been performed to probe the morphology of dissociative ionization of a ring molecule benzene when it is immersed in a laser field of 35-ps duration whose intensity is in the range  $10^{13} \text{ W cm}^{-2}$ . The field-induced fragmentation pattern is grossly different from that obtained by electron impact. The intense laser field clearly gives rise to much more fragmentation. Covariance mapping has been applied to study field-induced formation of highly charged molecular ions. Results indicate that the overall fragmentation dynamics is complex and is likely to involve both fast ladder switching as well as multiple ionization of fragment molecules at some intermediate steps in the ladder. Angular distributions of fragment ions have been measured. Anisotropic distributions indicate that some fragments are produced from precursors that are strongly aligned along the direction of the laser polarization vector while at least one fragment is formed from a precursor whose angular distribution is markedly isotropic. The nature of the precursors remains to be discovered. [S1050-2947(99)04202-X]

PACS number(s): 33.80.Rv, 33.80.Gj, 33.20.-t

### I. INTRODUCTION

There continues to be a paucity of information on the dynamical behavior of polyatomic molecules when they are immersed in short-duration, linearly polarized, light fields of intensity in excess of  $10^{12} \text{ W cm}^{-2}$ . At lower intensity levels, of the order of  $10^7$ – $10^{10} \text{ W cm}^{-2}$ , the last two decades have witnessed considerable progress in the development of laser-based mass spectrometry techniques, such as resonance ionization mass spectrometry (RIMS) and resonance-enhanced multiphoton ionization (REMPI). Both RIMS and REMPI have contributed immensely to successes in both fundamental and applied studies of the structural and dynamical properties of a gamut of atomic and polyatomic systems [1]. However, when higher laser intensities are used, such that their magnitudes begin to give rise to instantaneous electric fields that are comparable in magnitude to intramolecular Coulombic fields, nonlinear effects begin to dominate field-molecule interactions, and a host of new phenomena become important enough to have significant influence on the dynamics of molecular processes such as dissociative ionization.

Experiments have shown that nonlinear processes and dynamics, which have no analog in weak-field or zero-field situations, are responsible for phenomena such as the ejection of further electrons from the molecular core at internuclear separations far from equilibrium (multiple ionization), emission of high-energy photons (harmonic generation), above-threshold dissociation, enhanced ionization, and formation of very-high-energy above-threshold ionization electrons. Within the context of diatomic species, these intense-field-molecule interaction effects continue to attract considerable contemporary interest [2]. The intensity of the laser field also distorts molecular potential energy (PE) surfaces, and experimental manifestations of field-distorted, or “dressed,” PE curves include various nonlinear phenomena like above-threshold dissociation (attributable to diabatic or adiabatic crossings of PE curves [3]), bond-softening (brought about by suppression of the potential barrier against

dissociation in the vicinity of an avoided crossing [4]), and vibrational trapping (which occurs if a deep enough potential well is formed at large internuclear separations as a result of an avoided curve crossing [5]). Consideration of field-induced distortions of PE curves has also opened up the possibility of exercising some selectivity between these three competing processes in experiments, which utilize phase control in a two-color optical field [6]. Recently, attempts have also been made to probe the dissociation and ionization dynamics of polyatomic molecules by considering field-induced distortions of molecular electron-density distributions [7].

Any theoretical insight into the dynamics governing field-induced dissociative ionization of polyatomic molecules in linearly polarized, picosecond-long, light pulses has to account for one major distinctive feature: the spatial alignment of one or more bonds along the direction of the laser polarization vector. The possibility of spatially aligning molecules by means of linearly polarized, intense light fields has attracted much recent attention. It is established that the field associated with linearly polarized laser light of intensity greater than  $\sim 10^{12} \text{ W cm}^{-2}$  can induce sufficiently strong torques on an initially randomly oriented ensemble of linear diatomic and triatomic molecules such that dynamic alignment of the internuclear axes occurs. Experimental manifestations of such alignment are the anisotropic angular distributions of fragments produced upon subsequent dissociative ionization of such molecules: ion intensities are maximum in the direction of the laser polarization vector and minimum (frequently zero) in the orthogonal direction. Much of the interest in such alignment processes has been generated in the context of pendular-state spectroscopy [8,9] and coherent control [10].

Recently, experimental indications have been obtained that if the linearly polarized light field is of sufficiently short duration (say, of the order of 100 fs or less), dynamic alignment may not occur in molecules containing heavy atoms (such as iodine-containing diatomics and polyatomics) and the angular distributions of the products of dissociative ion-

ization in such cases might be determined by the dependence of the ionization rate on the angle made by the laser polarization vector with the molecule's symmetry axis (see, for instance, Ref. [11]). However, for intense light fields of longer duration (say, picoseconds and longer) and for most light molecules, the dynamics of field-induced spatial alignment is essentially governed by the molecular polarizability  $\alpha$ , which, in turn, is governed by a  $\cos^2\theta$  potential (as opposed to a  $\cos\theta$  potential applicable in the case of permanent dipoles). The total angular momentum of each molecule is coupled to the laser field through  $\alpha$ . The second-order field-molecule interaction potential  $V_\theta(\theta)$  is given by

$$V_\theta(\theta) = -\frac{1}{2}E^2(\alpha_{\parallel}\cos^2\theta + \alpha_{\perp}\sin^2\theta), \quad (1)$$

where  $E$  is the average field strength and  $\alpha_{\parallel}$  and  $\alpha_{\perp}$  are the polarizability components parallel to and perpendicular to the molecular bond. The  $V_\theta(\theta)$  term is, in general terms, the cause of the spatial alignment and earlier work [9] has shown that the field-molecule interaction energy overwhelms the field-free rotational energy and can thus induce alignment.

In the case of triatomic molecules possessing nonlinear equilibrium geometries (such as  $\text{NO}_2$ ,  $\text{H}_2\text{O}$ ,  $\text{SO}_2$ , . . .) it has been shown [12] that the ratio of the component of polarizability parallel to the molecular axis ( $\alpha_{\parallel}$ ) to that which lies in a perpendicular direction ( $\alpha_{\perp}$ ) determines the extent to which such molecules undergo spatial alignment when subjected to linearly polarized light of picosecond duration. For instance, in the case of  $\text{H}_2\text{O}$ , the values of  $\alpha_{\parallel}$  and  $\alpha_{\perp}$  are almost identical for a large range of laser intensities and, consequently, the angular distributions of  $\text{O}^+$  and  $\text{OH}^+$  fragments arising from field-induced dissociative ionization of water do not exhibit noticeable anisotropies. In contrast,  $\text{O}^+$  and  $\text{NO}^+$  fragments possess very anisotropic angular distributions as a result of  $\alpha_{\parallel}$  being significantly larger than  $\alpha_{\perp}$  in the case of  $\text{NO}_2$ .

For a polyatomic molecule the total polarizability ( $\alpha$ ) can be expressed as a sum of polarizabilities of the constituent groups [14]:

$$\alpha = \alpha_A + \alpha_B + \alpha_C + \dots, \quad (2)$$

where each of the constituent polarizabilities,  $\alpha_A, \dots$ , consist of two direction-dependent components,  $\alpha_{\parallel}$  and  $\alpha_{\perp}$ . If the applied electric field is at an angle  $\theta$  with a given bond in a polyatomic molecule, the polarizability  $\alpha_\theta$  is

$$\alpha_\theta = \alpha_{\parallel}\cos^2\theta + \alpha_{\perp}\sin^2\theta. \quad (3)$$

Averaging over all possible solid angles (spatial orientations) leads to an average value of the bond polarizability

$$\alpha' = \frac{1}{3}(\alpha_{\parallel} + 2\alpha_{\perp}). \quad (4)$$

The average polarizability of a polyatomic  $\alpha$  is then the sum of the average polarizabilities  $\alpha'$  of its bonds. Measurements of the angular distributions of the most intense fragment ion peak in mass spectra obtained upon intense-field-induced dissociative ionization (DI) of polyatomics such as  $\text{CCl}_4$ ,  $\text{CHCl}_3$ , and  $\text{CH}_2\text{Cl}_2$  have shown that spatial alignment

does occur in these nonlinear molecules [13]. It has been shown that the magnitude of the linear polarizability of such molecules is, in itself, not a sufficiently useful parameter for predicting the degree of spatial alignment; the directional properties of the polarizability play a key role. This is exemplified by the ratio of  $\alpha_{\parallel}$  of the *most polarizable* bond in the polyatomic molecule to the *total* polarizability [13]. This ratio is clearly dependent on molecular symmetry. It is also related, in complex fashion, to the torque that might be expected to be exerted on the molecule as a result of the interaction of the applied laser field with the most polarizable of the many bonds in a polyatomic molecule.

It is the purpose of this paper to report results of experiments that extend the recent studies on intense-field interactions with tetrahedral  $\text{CCl}_4$  and substituted chloromethanes to a polyatomic species possessing a cyclic geometry. Benzene is the obvious prototype ring molecule and is the focus of attention in this study. We describe in the following results of a morphological study of the DI pattern obtained when  $\text{C}_6\text{H}_6$  is immersed in light fields of intensity in the range  $10^{13} \text{ W cm}^{-2}$ , wavelength of 532 nm and pulse duration of 35 ps. Angular distributions of fragments resulting from DI of  $\text{C}_6\text{H}_6$  have been measured. Field-induced multiple ionization has also been probed using the covariance mapping technique.

## II. EXPERIMENTAL METHOD

Our experiments were conducted using apparatus and methodology that have been described in recent reports of DI and angular distribution measurements of a number of triatomic molecules [9,15]. In brief, linearly polarized, 35-ps-wide, 532-nm pulses from an Nd:YAG (yttrium aluminum garnet) laser, focused to a spot size of 25  $\mu\text{m}$  [15], interacted with benzene vapor maintained at pressures of  $\sim 10^{-6}$  Torr. The benzene used was of analytical grade; it was degassed by means of several freeze-pump-thaw cycles in a clean, greaseless vacuum line. Typical laser intensities used were in the range  $1-8 \times 10^{13} \text{ W cm}^{-2}$ . Ions produced in the laser-molecule interaction were mass analyzed either by a quadrupole mass spectrometer or, in a different apparatus, by means of a linear time-of-flight mass spectrometer; in both cases ion detection was by a channel electron multiplier operating in the particle counting mode.

Angular distributions of fragment ions were measured by rotating the polarization direction of the incoming laser field with respect to the spectrometer axis; a combination of half-wave plate and linear polarizer was used to obtain the desired polarization at constant intensity. The shot-to-shot reproducibility of the laser intensity was  $\pm 5\%$ ; this was ensured by on-line monitoring of the laser energy [16]. Only those ions whose initial velocity vector lay within the acceptance angle set by the entrance aperture of the mass filter were detected; the angular resolution was approximately  $4^\circ$  in both the apparatuses used in the present measurements. A detailed discussion has recently been presented of how fragment ion angular distributions are affected by charge saturation effects [17] when large target gas number densities are used [16]. As noted above, our angular distribution measurements were made under conditions such that the number density of  $\text{C}_6\text{H}_6$

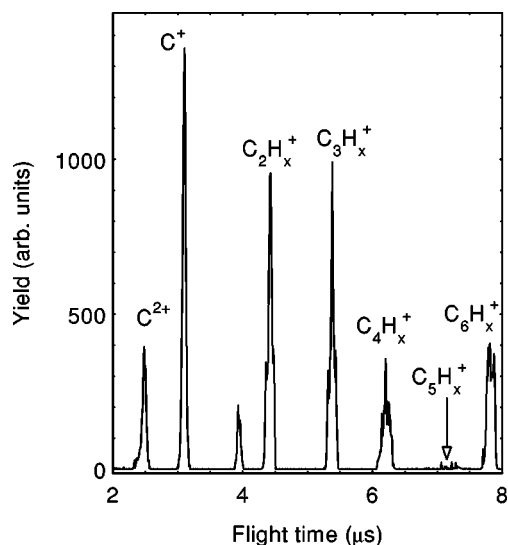


FIG. 1. Time-of-flight mass spectrum obtained upon irradiation of benzene by 532-nm, linearly polarized light of intensity  $4 \times 10^{13} \text{ W cm}^{-2}$ . The measurement was made at an operating gas pressure of  $8 \times 10^{-7}$  Torr, with the laser polarization vector lying parallel to the spectrometer axis.

molecules in laser focal volume was low enough to obviate the need for us to explicitly consider space-charge effects.

### III. RESULTS AND DISCUSSION

#### A. Morphology of dissociative ionization

Figure 1 shows a typical time-of-flight spectrum obtained when  $\text{C}_6\text{H}_6$  was irradiated by 532-nm light of intensity  $4 \times 10^{13} \text{ W cm}^{-2}$ . The benzene vapor pressure in the interaction zone was  $8 \times 10^{-7}$  Torr. It is instructive to note the differences between the laser-field-induced DI pattern and that obtained in electron-impact experiments conducted at a collision energy of 70 eV (see Fig. 2). The  $\text{C}_6\text{H}_6^+$  parent ion dominates the electron-impact spectrum shown in Fig. 2, and fragments smaller than  $\text{C}_2\text{H}_x^+$  contribute only very marginally to the spectrum. The field-induced spectrum in Fig. 1 shows  $\text{C}^+$  as the dominant ion peak with the  $\text{C}_6\text{H}_6^+$  parent ion being only a relatively minor constituent of the mass spectrum. The intense laser field clearly gives rise to much more fragmentation. In this respect, our picosecond laser experiments appear to yield a mass spectrum that is qualitatively similar to that obtained in earlier experiments, mostly conducted at much lower field magnitudes ( $\sim 10^8 \text{ W cm}^{-2}$ ) and using femtosecond [18] and nanosecond duration pulses [19–21]. This qualitative agreement appears to hold independently of wavelength considerations as a very wide wavelength range was covered in these four earlier experiments. The measurements of DeWitt and Levis [18] were made using infrared light pulses of 170-fs duration. On the other hand, the experiments of Reilly and Kompf [19], and of Schlag and co-workers [20], were conducted using ultraviolet light pulses of 12–20-ns duration whereas Zandee and Bernstein [21] used somewhat higher laser intensities ( $\sim 10^{10} \text{ W cm}^{-2}$ ) and a near-visible dye laser.

All these earlier data sets indicated enhanced fragmentation compared to the electron-impact case, with little or no

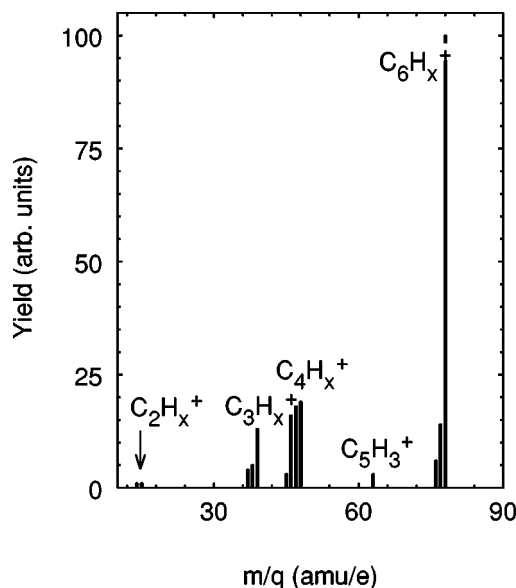


FIG. 2. Mass spectrum of benzene measured using 70-eV electrons.

multiple ionization in the laser experiments. These observations indicated, somewhat unexpectedly, that despite the intrinsic strength of its aromatic ring structure, benzene does not multiply ionize but, rather, it fragments in the course of interactions with strong light fields. Our picosecond experiments, which utilize much stronger light fields and visible photons, still lie within the multiphoton regime and essentially reproduce the gross features of the fragmentation patterns observed in the earlier measurements. Does our fragmentation pattern result from dissociation of an electronically excited state of  $\text{C}_6\text{H}_6^+$ , which is formed after several additional photons are absorbed by the molecular ions? Or, is a series of successive field-induced fragmentation and ionization steps responsible for the mass spectra measured in our experiments? Both scenarios are possible if one considers that following the initial ejection of a single electron from neutral benzene, the molecular ion continues to be subjected to intense laser radiation and, consequently, undergoes further interactions with the light field. The duration of the laser pulse is clearly a parameter of some importance in considering the time scales of possible unimolecular dissociation processes of highly excited states of  $\text{C}_6\text{H}_6^+$ . Unimolecular process such as  $[\text{C}_6\text{H}_6^+ \rightarrow \text{fragment ions}]$  would occur on short time scales. Thus some unimolecular dissociation might be expected to compete with photon absorption when laser pulses of nanosecond duration are used. However, 35-ps-long pulses might be considered short enough to ensure that successive photon absorption is the more likely route to enhanced fragmentation of benzene. On the basis of their nanosecond experiments, Schlag and co-workers [20] characterized this successive photon absorption process as “ladder switching”: fast unimolecular processes produce switching of the excitation ladder into fragments. A schematic representation of ladder switching applied to benzene is depicted in Fig. 3. After initial ejection of an electron from neutral  $\text{C}_6\text{H}_6$ , the field- $\text{C}_6\text{H}_6^+$  interaction results in the following sequence: (i) further excitation of the molecular ion; (ii) dissociation of an excited state of  $\text{C}_6\text{H}_6^+$  into, say,  $\text{C}_4\text{H}_x^+$

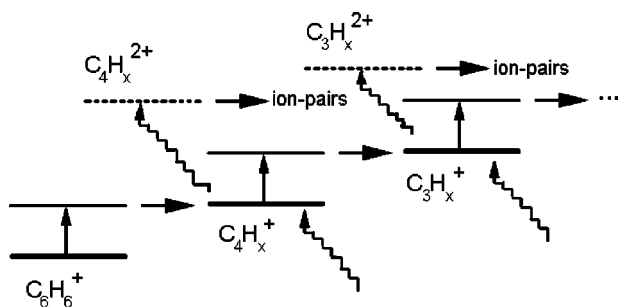


FIG. 3. Schematic representation of a modified ladder-switching mechanism (see text). The vertical arrows indicate multiphoton excitation while the horizontal arrows indicate dissociation of excited ionic states. The dissociation products can themselves interact with the laser light (diagonal curly arrows) and undergo double (or multiple) ionization, and such product states are indicated by dashed horizontal lines. These highly charged states unimolecularly decay into ion pairs that can be experimentally detected by multiple coincidence techniques such as covariance mapping (see Fig. 6).

+ neutral fragments; (iii) excitation of  $C_4H_x^+$ ; (iv) dissociation of an excited state of  $C_4H_x^+$  into, say,  $C_2H_x^+$  + neutral fragments; and so on, until  $C^+$  is ultimately produced.

Does the ladder switching mechanism apply to field- $C_6H_6^+$  interactions when laser pulses are used, which are of only 35-ps duration? Or, alternatively, can the fragmentation patterns that we measure be attributed to field-induced distortions of the potential energy surface of an excited state of  $C_6H_6^+$ ? We consider the latter alternative unlikely in light of the larger yield of smaller fragments that are observed in our mass spectra. It appears improbable that our fragmentation pattern could result from a single explosion of one, highly excited, field-distorted state of  $C_6H_6^+$ . Moreover, simple energetic considerations also appear to favor the first alternative. It is pertinent to note in this connection the nonobservation in earlier measurements [18–20] of metastable  $C_6H_6^{2+}$  dications, which have an appearance energy of  $\sim 26$  eV, while copious yields were obtained of fragment ions such as  $C_3H_x^+$ ,  $C_2H_x^+$ , and  $C^+$  whose appearance energies are as high as 30–45 eV. It is difficult to postulate a single explosion of a field-excited state of  $C_6H_6^+$  that would account for such energetically unfavorable fragmentation routes, apparently at the expense of lower-energy double-ionization channels.

### B. Field-induced multiple ionization

Can part of the observed fragmentation pattern be accounted for in terms of fast unimolecular dissociation of multiply ionized benzene (or some of its fragments) as opposed to singly ionized benzene? To probe this, we used our time-of-flight (TOF) spectrometer to make covariance maps in order to probe temporal correlations between ion pairs, which might arise upon spontaneous fragmentation of  $C_xH_x^{q+}$  ( $q \geq 2$ ) ions. In our experiment the output pulses from the channel electron multiplier were amplified and fed into a fast digital storage oscilloscope (DSO) coupled to a computer through a fast data bus. The sampling rate of the DSO was  $0.5 \times 10^9$  per second, with an analog bandwidth of 100 MHz. Typically, mass spectra were accumulated over 20 000–30 000 laser shots; the times of arrival of ions pro-

duced in each laser shot were recorded by the DSO and stored in a computer's memory for off-line analysis using the covariance mapping technique. Covariance mapping is a general technique utilized in diverse areas of physics research to reveal hidden correlations in highly fluctuating signals. Frasniski and co-workers [22] have extensively utilized the technique to study the fragmentation dynamics of multiply charged, positive ions of small molecules; we have also utilized this technique in recent experiments on highly charged  $CS_2$  ions and negatively charged carbon clusters [23]. In this technique, the TOF spectrum is represented as  $X(t_1)$  at 1000 discrete points where  $X(t_1)$  represents a 1000-element vector indexed by  $t$ . If  $Y(t_2)$  is the same vector, the covariance matrix  $C(t_1, t_2)$  between each pair of TOF points  $t_1$  and  $t_2$  can be obtained from the tensor product:

$$\begin{aligned} C(t_1, t_2) &= \langle (X - \langle X \rangle)(Y - \langle Y \rangle) \rangle = \langle XY \rangle - \langle X \rangle \langle Y \rangle \\ &= \langle X(t_1)Y(t_2) \rangle - \langle X(t_1) \rangle \langle Y(t_2) \rangle. \end{aligned} \quad (5)$$

For averages taken over a total of  $N$  laser pulses (typically 20 000–30 000),

$$\begin{aligned} C(t_1, t_2) &= \frac{1}{N} \sum_{i=1}^N X_i(t_1)Y_i(t_2) \\ &\quad - \left[ \frac{1}{N} \sum_{i=1}^N X_i(t_1) \right] \left[ \frac{1}{N} \sum_{i=1}^N Y_i(t_2) \right]. \end{aligned} \quad (6)$$

The map of covariances is the small difference between two large correlated ( $\langle XY \rangle$ ) and uncorrelated ( $\langle X \rangle \langle Y \rangle$ ) products and is a measure of the temporal correlations between ion pairs in TOF spectra. The ion collection efficiency must approach 100% in order for covariance mapping to yield statistically reliable results. In the present experimental configuration we measured the intensity of different fragment ions as a function of the magnitude of the electrostatic field used to extract ions into our TOF spectrometer. Our results indicate that at field values in excess of  $\sim 100$  V  $cm^{-1}$ , unit collection efficiency was achieved (as indicated by saturation of the ion yield when plotted as a function of extraction field). The covariance map measured in our experiments were all obtained using extraction fields of the order of 200 V  $cm^{-1}$ .

Part of a typical map showing coincidences involving different fragment ions is depicted in Fig. 4. The peaks represent true coincidence signals arising from *correlated* ion pairs. The autocorrelation signal has also been removed in order to improve visual clarity. We have divided the map into three different sets of ion pairs on the basis of the strength of the covariance signal. The group possessing maximum intensities in the covariance maps comprise  $C^+ + C_2H_x^+$ ,  $C^+ + C_3H_x^+$ , and  $C_2H_x^+ + C_3H_x^+$ . The medium-intensity group consist of  $C^+ + C_4H_x^+$  and  $C_4H_x^+ + C_2H_x^+$  ion pairs whereas the lowest-intensity ion pairs are  $C^+ + C^{2+}$ ,  $C^{2+} + C_2H_x^+$ ,  $C^{2+} + C_3H_x^+$  and  $C^{2+} + C_4H_x^+$ .

It is noteworthy that of the large number of possible ion pairs whose formation may be postulated upon dissociation of  $C_6H_6^{q+}$  ( $q \geq 2$ ), only the above-noted nine pairs were evident in our covariance map. Nevertheless, covariance maps accumulated by us at different laser intensities indicate in an

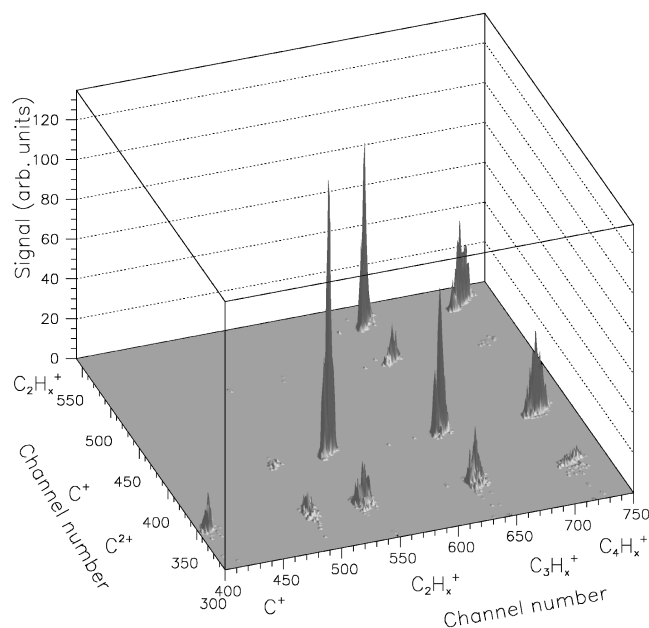


FIG. 4. Part of a covariance map showing time-correlated ion pairs produced by multiple ionization induced by a laser field of intensity  $1 \times 10^{13} \text{ W cm}^{-2}$ . The autocorrelation line has been artificially removed in order to improve clarity. The channel numbers are proportional to ion time of flight.

unambiguous fashion that multiply charged molecular ions do get formed under our experimental conditions of picosecond laser irradiation. The earlier claims [18–21] that multiple ionization does not occur constituted a major factor in support of the ladder switching mechanism. These nonobservations of multiple ionization were based on measurements of “singles” mass spectra and pertained only to the absence of long-lived doubly and triply charged molecular ions. The application of the covariance mapping technique has enabled us to probe the formation of *short-lived* dications and trications and it is clear that such species must be considered in any dynamical model which seeks to rationalize the fragmentation pattern obtained when benzene interacts with intense laser light. In light of the earlier discussion of the possible role of ladder switching in determining the fragmentation dynamics, it is important to note the following. The observation that almost all the ion pairs that are found to contribute to our covariance map involve atomic ions,  $\text{C}^+$  or  $\text{C}^{2+}$ , offers an indication that the overall dynamics is complex in that it is likely to involve both fast ladder switching as well as a measure of multiple ionization of fragment molecules at some intermediate steps in the ladder. More work clearly needs to be undertaken in order to gain better insight.

### C. Angular distributions of fragment ions

Angular distributions of fragment ions were measured using the TOF spectrometer as well as with a quadrupole mass spectrometer. The acceptance angle of our TOF spectrometer is dependent on the kinetic energy of the ions formed in the laser-molecule interaction zone. We carried out ion trajectory calculations for our operating conditions; the variation of our instrument’s acceptance angle with ion kinetic energy is de-

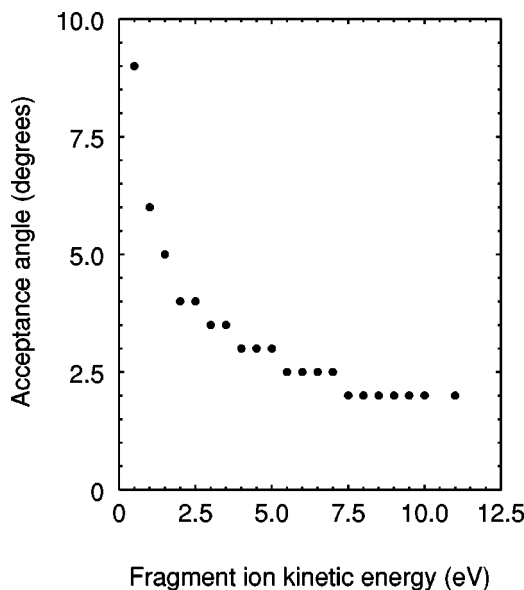


FIG. 5. Computer simulations of ion trajectories showing the dependence of the acceptance angle (half width at half maximum) of our time-of-flight spectrometer on the fragment ion kinetic energy.

picted in Fig. 5. The largest kinetic energy with which different ion pairs are formed was  $\sim 3.5 \text{ eV}$ ; such ions were detected with an acceptance angle of  $\sim 3^\circ$  (half angle at half width). When the quadrupole mass spectrometer was employed, angular distributions could be measured with zero ion extraction voltage. This afforded the possibility of measuring pristine angular distributions, unaffected by distortions that may be induced by ion extraction fields in the laser-molecule interaction zone. In such cases, the ion acceptance angle was the same as the geometrical acceptance angle and, in our instrumental configuration, this value was  $4^\circ$  (half angle at half width).

Figure 6 shows typical angular distributions measured for  $\text{C}^+$  fragment ions at a laser intensity of  $2.4 \times 10^{13} \text{ W cm}^{-2}$ . The data are presented as a polar plot, with the radial distance from the origin of each data point being a measure of ion yield in a given angular direction. A number of angular distribution measurements were made which, taken together, covered all four quadrants in the angular

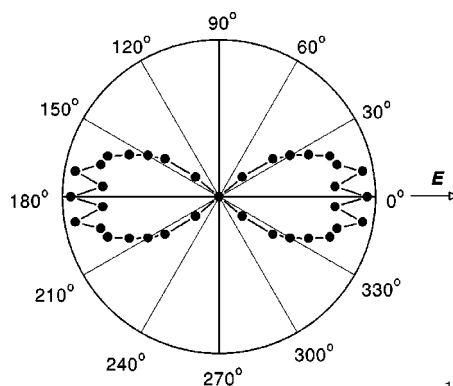


FIG. 6. Polar plot showing the angular distribution of  $\text{C}^+$  fragment ions. The measurements were made using a laser intensity of  $2.4 \times 10^{13} \text{ W cm}^{-2}$ .

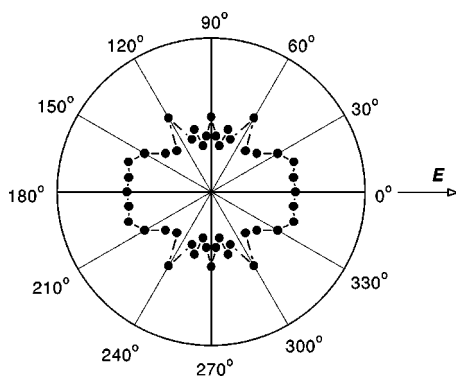


FIG. 7. Polar plot showing the angular distribution of  $C_2H_x^+$  fragment ions. The measurements were made using a laser intensity of  $5 \times 10^{13} \text{ W cm}^{-2}$ .

range  $0^\circ$ – $360^\circ$  around the spectrometer axis. As in other recent work reported from our laboratory [12,13,15,16], no difference was found in the shapes of the distributions obtained in the different quadrants when the alignment of the focused laser beam with the molecular target and the spectrometer axis was perfect. The angular distribution data depicted in Fig. 6 pertain to measurements made in the  $0^\circ$ – $90^\circ$  quadrant; for clarity of presentation, we have chosen to reflect such single quadrant data over the  $90^\circ$ – $360^\circ$  range.

The anisotropy of the fragment ion signal would be expected to be dependent on the vector properties of field-induced transition moments associated with intermediate excited states of the precursor and their relation to the direction of the laser polarization vector. Distributions of the form  $\cos^n \theta$  and  $\sin^n \theta$  result from  $n$ -photon excitations, producing major lobes at  $0^\circ, 180^\circ$  and minor ones at  $90^\circ, 270^\circ$ ; contributions from a  $\cos \theta \sin \theta$  type of angular function result in lobes at  $\sim 60^\circ, 120^\circ, 240^\circ$ , and  $300^\circ$  (for discussion of such vector correlations, see [24,25]). The polar plot shown in Fig. 6 is clearly not amenable to simple interpretation in terms of conventional vector correlation models; the data offer indications of spatial alignment of precursors that give rise to the pronounced anisotropies observed in the angular distributions measured for  $C^+$  fragment ions. The ion yield at  $90^\circ$  was measured to be zero. Our measurements offered some indications of structure in the polar plots that was found to be reproducible, in the vicinity  $5^\circ$ – $15^\circ$ . Earlier observations of such structure in angular distributions of fragment ions from field-induced dissociative ionization of triatomics like  $CS_2$  and  $CO_2$  have been interpreted in terms of formation of pendular states [9]. In the present case we consider it imprudent to ascribe the observed structure to a similar phenomenon, particularly in the absence of definitive evidence of the nature of the immediate precursors of the  $C^+$  fragments.

Figure 7 shows angular distribution data for  $C_2H_x^+$  fragments obtained. This measurement was made at a laser intensity of  $5 \times 10^{13} \text{ W cm}^{-2}$ . Measurements on this fragment were made using both our TOF spectrometer as well as the quadrupole mass spectrometer. In contrast to data shown in Fig. 6,  $C_2H_x^+$  fragment ions are clearly formed with an angular distribution that is markedly more isotropic.

#### IV. SUMMARY AND CONCLUDING REMARKS

We have carried out mass spectrometry experiments to probe the morphology of dissociative ionization of a ring molecule, benzene, when it is immersed in an intense laser field (intensity in the range  $10^{13} \text{ W cm}^{-2}$ ) of 35-ps duration. The following features of the dynamics of field-induced DI emerge out of our measurements.

(i) The field-induced fragmentation pattern is dramatically different from that obtained in conventional electron-impact mass spectrometry. Whereas the  $C_6H_6^+$  parent ion dominates the electron-impact spectrum, and fragments smaller than  $C_2H_x^+$  contribute only very marginally to the overall fragmentation pattern, field-induced spectra show  $C^+$  as the dominant fragment, with the  $C_6H_6^+$  parent ion being only a relatively minor constituent of the mass spectrum. The intense laser field clearly gives rise to much more fragmentation. Our picosecond laser experiments yield a mass spectrum which is qualitatively similar to that obtained in earlier experiments conducted at lower field magnitudes using nanosecond pulses [18–21]. This apparent similarity of fragmentation pattern appears to hold independent of wavelength considerations. In the light of earlier suggestions of a ladder switching mechanism [20], the following sequence of events can be postulated: After initial ejection of an electron from neutral  $C_6H_6$ , the field- $C_6H_6^+$  interaction results in further excitation of the molecular ion  $\rightarrow$  followed by dissociation of an excited state of  $C_6H_6^+$  into, say,  $C_4H_n^+$  + neutral fragments  $\rightarrow$  excitation of  $C_4H_n^+$   $\rightarrow$  dissociation of an excited state of  $C_4H_n^+$  into, say,  $C_2H_n^+$  + neutral fragments  $\rightarrow$  and so on, until  $C^+$  is ultimately produced. Qualitatively, it is possible to state that the fragmentation pattern is determined by charge transfer type of couplings between adjacent molecular orbitals that are accessed in the course of unexpectedly fast ladder switching that appears to occur while the laser pulse is on. Our data indicate that such internal conversion between different excited states within the ladder appears to occur on a timescale which may be significantly shorter than 35 ps. Our results indicate that the sequence of events we have postulated here in the context of ladder switching needs to be enhanced in scope, as discussed in the following.

(ii) The gross features of the mass spectra were found to be only weakly dependent on laser intensity, at least over the range  $1$ – $8 \times 10^{13} \text{ W cm}^{-2}$ .

(iii) Multiple ionization is a process that would need to be incorporated into the ladder switching sequence of events postulated in (i). Our covariance maps revealed that only a small subset of the large number of possible ion pairs, whose formation may be postulated upon dissociation of  $C_6H_6^{q+}$  ( $q \geq 2$ ), were evident in our covariance map. The most prominent ion pairs to be detected were  $C^+ + C_2H_x^+$ ,  $C^+ + C_3H_x^+$ , and  $C_2H^+ + C_3H_x^+$ , indicating the likely formation of highly charged precursors that are smaller in size than the parent  $C_6H_6$  molecule. The observation that almost all the ion pairs that were found to contribute to our covariance map involved atomic ions,  $C^+$  or  $C^{2+}$ , might indicate that the complex dynamics is likely to involve both fast (modified) ladder switching as well as multiple ionization of fragment molecules at some intermediate steps in the ladder. Conventional ladder switching mechanisms de-

mand a rapid increase with internal energy of unimolecular dissociation rates. Consequently, the parent ion dissociates before additional photons are absorbed. This is the justification for the nonobservation of metastable multiply charged ions and the observed intensity dependence of the DI patterns in earlier long-pulse experiments. In the present, shorter-pulse measurements, the rates for unimolecular dissociation seem to be comparable to those for absorption of additional photons; hence, the measured independence of the DI pattern with laser intensity in our experiments. There are grounds to justify consideration of a modification to the conventional ladder-switching mechanism by incorporating the possibility of the occurrence of some measure of ladder climbing in our short-pulse experiments.

(iv) The angular distributions measured for  $C^+$  fragment ions show very pronounced anisotropies, with zero ion yield obtained when the laser polarization direction is orthogonal to the spectrometer axis. These anisotropies are indicative of

field-induced spatial alignment of the precursors. On the other hand, our data also indicate that  $C_2H_x^+$  fragment ions are formed with an angular distribution that is markedly more isotropic. The precursor for  $C^+$  on the one hand and for  $C_2H_x^+$  on the other appear to possess significantly different geometries. The former have anisotropic molecular polarizabilities such that one of the bonds becomes spatially aligned along the direction of the laser polarization vector. In the latter case, the precursor appears to have a geometry that is such that field-induced dipole moments do not create a net torque, which results in spatial alignment in a particular direction. The nature of the precursors remains to be discerned.

#### ACKNOWLEDGMENTS

We are grateful to M. Krishnamurthy for incisive comments on our manuscript, and for helpful discussions.

- 
- [1] G. I. Bekov and V. S. Letokhov, *Appl. Phys. B: Photophys. Laser Chem.* **B30**, 161 (1983); G. S. Hurst and V. S. Letokhov, *Phys. Today* **47** (4), 38 (1994).
- [2] E. Constant, H. Stapelfeldt, and P. B. Corkum, *Phys. Rev. Lett.* **76**, 4140 (1996); *Molecules in Laser Fields*, edited by A. D. Bandrauk (Dekker, New York, 1993); J. L. Krause, K. J. Schaffer, and K. C. Kulander, *Phys. Rev. Lett.* **68**, 3535 (1992); P. B. Corkum, *ibid.* **71**, 1994 (1993); M. Yu. Kuchiev, *Phys. Lett. A* **212**, 77 (1996); A. Becker and F. H. M. Faisal, *J. Phys. B* **29**, L197 (1996), and references therein.
- [3] A. Giusti-Suzor, F. H. Mies, L. F. DiMauro, E. Charron, and B. Yang, *J. Phys. B* **28**, 309 (1995).
- [4] P. H. Bucksbaum, A. Zavriyev, H. G. Muller, and D. W. Schumacher, *Phys. Rev. Lett.* **64**, 1883 (1990).
- [5] J. E. Decker, G. Xu, and S. L. Chin, *J. Phys. B* **24**, L281 (1991).
- [6] H. G. Muller, P. H. Bucksbaum, D. W. Schumacher, and A. Zavriyev, *J. Phys. B* **23**, 2761 (1990); D. W. Schumacher, F. Weihe, H. G. Muller, and P. H. Bucksbaum, *Phys. Rev. Lett.* **73**, 1344 (1994); B. Sheehy, B. Walker, and L. F. DiMauro, *ibid.* **74**, 4799 (1995).
- [7] K. Vijayalakshmi, V. R. Bhardwaj, C. P. Safvan, and D. Mathur, *J. Phys. B* **30**, L339 (1997); K. Vijayalakshmi, V. R. Bhardwaj, and D. Mathur, *ibid.* **30**, 4065 (1997).
- [8] B. Friedrich and D. Herschbach, *Phys. Rev. Lett.* **74**, 4623 (1995).
- [9] G. R. Kumar, P. Gross, C. P. Safvan, F. A. Rajgara, and D. Mathur, *Phys. Rev. A* **53**, 3098 (1996); *J. Phys. B* **29**, L95 (1996).
- [10] E. Charron, A. Giusti-Suzor, and F. H. Mies, *Phys. Rev. A* **49**, R641 (1994).
- [11] J. H. Posthumus, J. Plumridge, M. K. Thomas, K. Codling, L. J. Frasinski, A. J. Langley, and P. F. Taday, *J. Phys. B* **31**, L553 (1998).
- [12] V. R. Bhardwaj, C. P. Safvan, K. Vijayalakshmi, and D. Mathur, *J. Phys. B* **30**, 3821 (1997).
- [13] V. R. Bhardwaj, K. Vijayalakshmi, and D. Mathur, *Phys. Rev. A* **56**, 2455 (1997); D. Mathur and K. Vijayalakshmi, *Rapid Commun. Mass Spectrom.* **12**, 246 (1998).
- [14] J. O. Herschfelder, C. F. Curtiss, and R. B. Bird, *Molecular Theory of Gases and Liquids* (Wiley, New York, 1954), p. 949.
- [15] G. R. Kumar, C. P. Safvan, F. A. Rajgara, and D. Mathur, *J. Phys. B* **27**, 2981 (1994); *Chem. Phys. Lett.* **217**, 626 (1994); K. Vijayalakshmi, V. R. Bhardwaj, C. P. Safvan, and D. Mathur, *J. Phys. B* **30**, L339 (1997).
- [16] C. P. Safvan, R. V. Thomas, and D. Mathur, *Chem. Phys. Lett.* **286**, 329 (1998); D. Mathur, V. R. Bhardwaj, P. Gross, G. R. Kumar, F. A. Rajgara, C. P. Safvan, and K. Vijayalakshmi, *Laser Phys.* **7**, 829 (1997).
- [17] M. V. Ammosov, F. A. Il'kov, M. G. Malakhov, and Ch. K. Mukhtarov, *J. Opt. Soc. Am. B* **6**, 1961 (1989).
- [18] M. J. DeWitt and R. J. Levis, *J. Chem. Phys.* **102**, 8670 (1995).
- [19] J. P. Reilly and K. L. Kompa, *J. Chem. Phys.* **73**, 5468 (1980).
- [20] H. J. Neusser, U. Boesl, R. Weinkauff, and E. W. Schlag, *Int. J. Mass Spectrom. Ion Processes* **60**, 147 (1984); U. Boesl, H. J. Neusser, and E. W. Schlag, *Chem. Phys. Lett.* **87**, 1 (1982).
- [21] L. Zandee and R. B. Bernstein, *J. Chem. Phys.* **70**, 2574 (1979); **71**, 1359 (1979).
- [22] L. J. Frasinski, K. Codling, and P. A. Hatherly, *Science* **246**, 1029 (1987); P. A. Hatherly, L. J. Frasinski, K. Codling, A. J. Langley, and W. Shaikh, *J. Phys. B* **23**, L291 (1990).
- [23] C. P. Safvan, V. R. Bhardwaj, G. R. Kumar, D. Mathur, and F. A. Rajgara, *J. Phys. B* **29**, 3135 (1996); D. Mathur, V. R. Bhardwaj, F. A. Rajgara, and C. P. Safvan, *Chem. Phys. Lett.* **277**, 558 (1997).
- [24] R. Shinke, *Photodissociation Dynamics* (Cambridge University Press, Cambridge, 1993).
- [25] C. P. Safvan, K. Vijayalakshmi, F. A. Rajgara, G. R. Kumar, V. R. Marathe, and D. Mathur, *J. Phys. B* **29**, L481 (1996).